Electronic Supplementary Material (ESI) for Polymer Chemistry.

Supporting Information for *Polymer Chemistry* article:

Tuning the Vesicle-to-Worm Transition for Thermoresponsive Block Copolymer Vesicles Prepared via Polymerisation-Induced Self-Assembly

Isabella R. Dorsman, Matthew J. Derry, Victoria J. Cunningham,

Steven L. Brown, Clive N. Williams and Steven P. Armes*

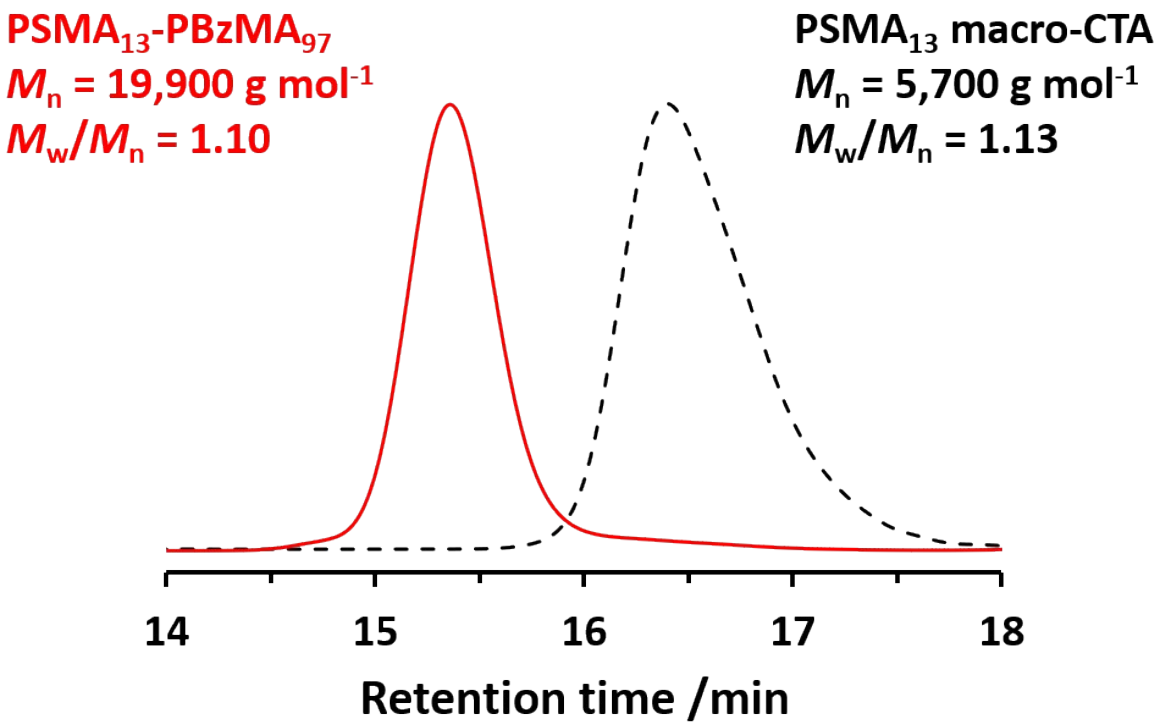

Fig. S1 THF GPC traces recorded for $PSMA_{13}$-$PBzMA_{97}$ diblock copolymer chains and the corresponding $PSMA_{13}$ macro-CTA precursor.

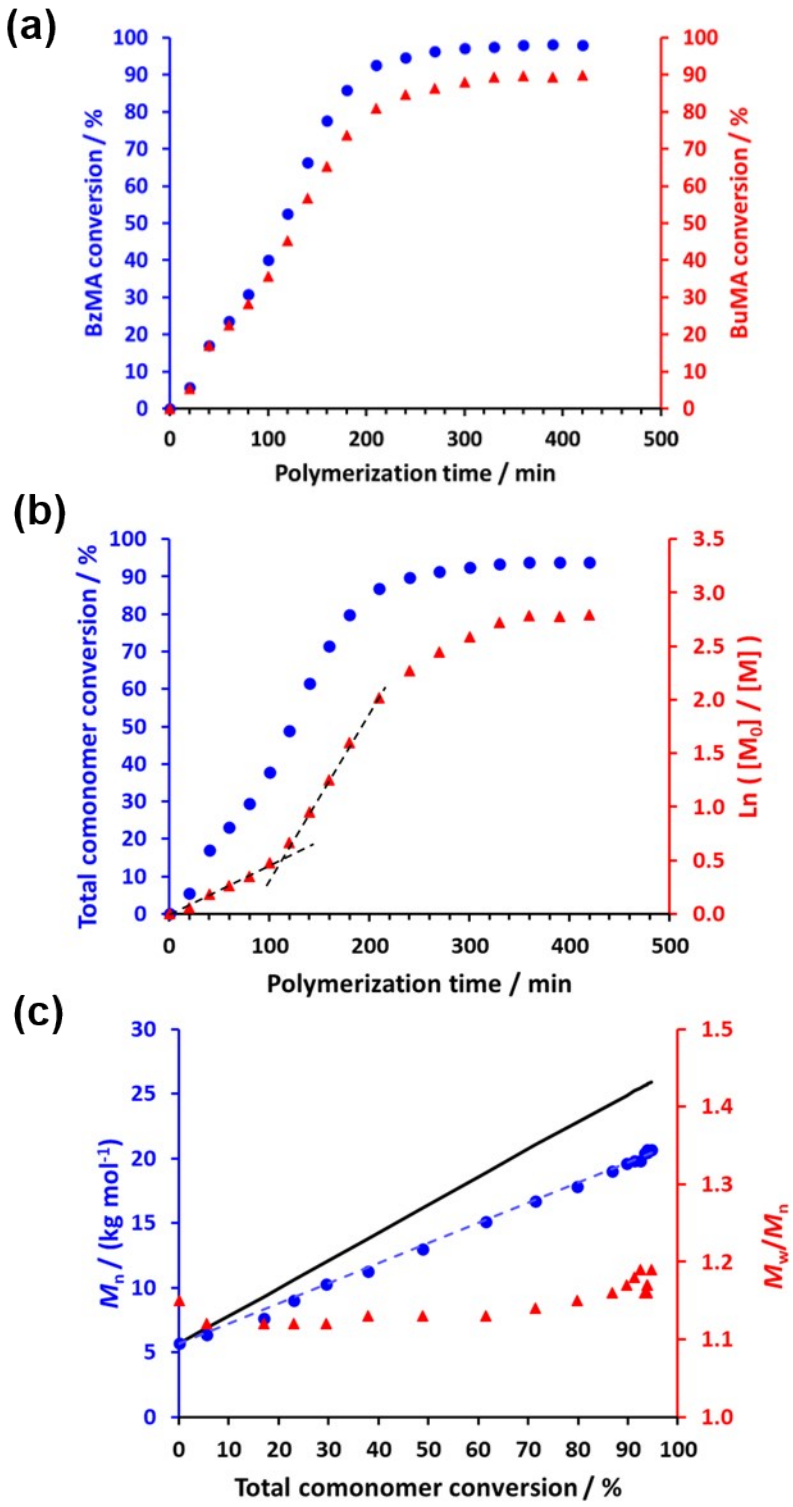

Fig. S2 (a) BzMA monomer conversion vs. time curve (blue circles) and BuMA monomer conversion vs. time curve (red triangles). (b) Overall comonomer conversion vs. time curve (blue circles) and corresponding $\ln([M]_0/[M])$ *vs.* time (red triangles) plot. (c) Evolution in M_n (blue circles) and M_w/M_n (red triangles) with comonomer conversion during the synthesis of $PSMA_{14}$-P(0.5BzMA-*stat*-0.5BuMA)$_{130}$ nanoparticles via RAFT dispersion copolymerization of BzMA with BuMA at 90 °C when targeting 10% w/w solids in mineral oil. The theoretical M_n *vs.* overall comonomer conversion relationship is indicated by the black solid line for this series, with the difference being attributed to the systematic error incurred by using a series of poly(methyl methacrylate) calibration standards.

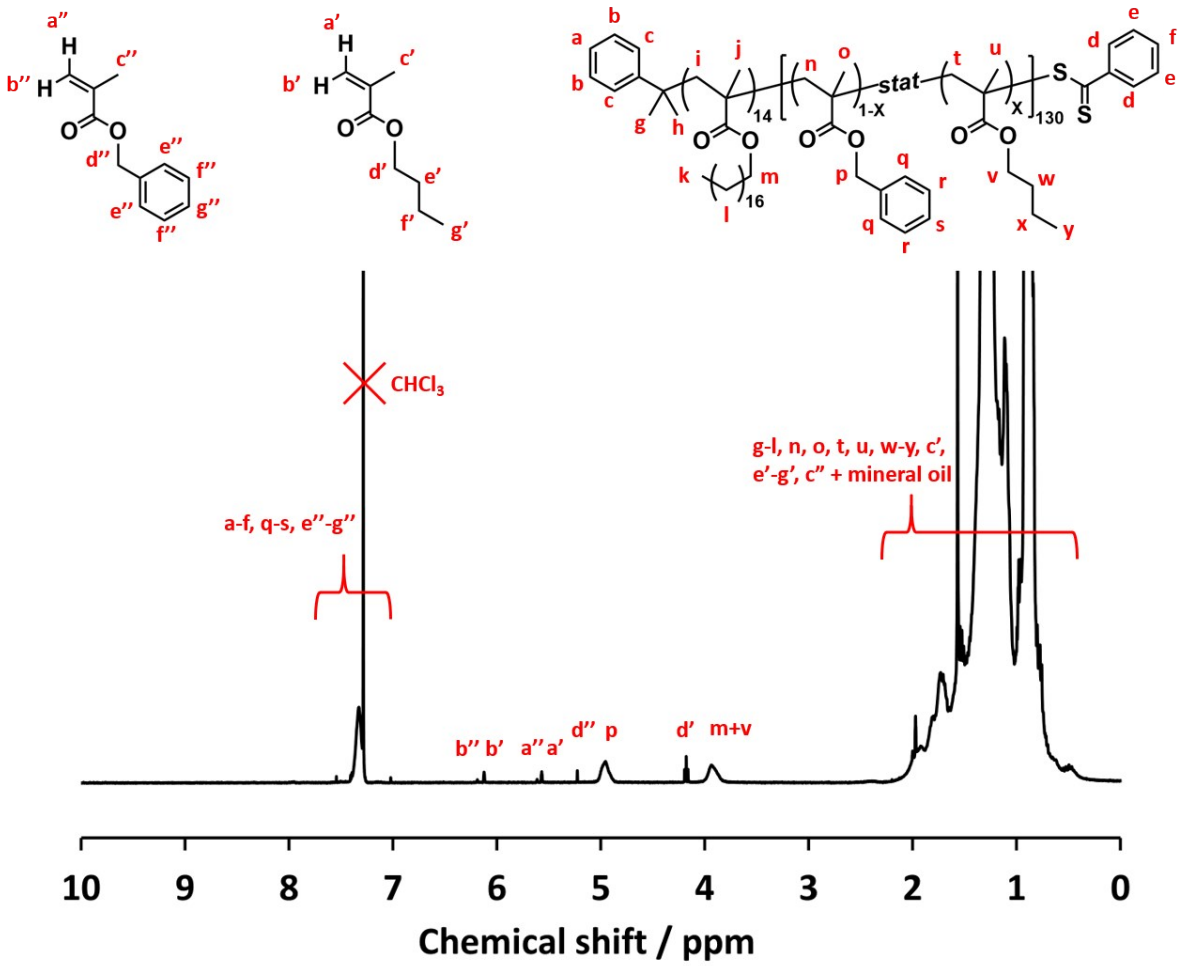

Fig. S3 Assigned ^{1}H NMR spectrum (recorded in $CDCl_3$) obtained for the reaction mixture directly after the synthesis of $PSMA_{14}$-P(0.5BzMA-*stat*-0.5BuMA)$_{130}$ nano-objects via RAFT dispersion copolymerization of BzMA with BuMA at 90 °C when targeting 10% w/w solids in mineral oil. [N.B. The nano-objects formed in mineral oil become molecularly dissolved in the presence of $CDCl_3$].

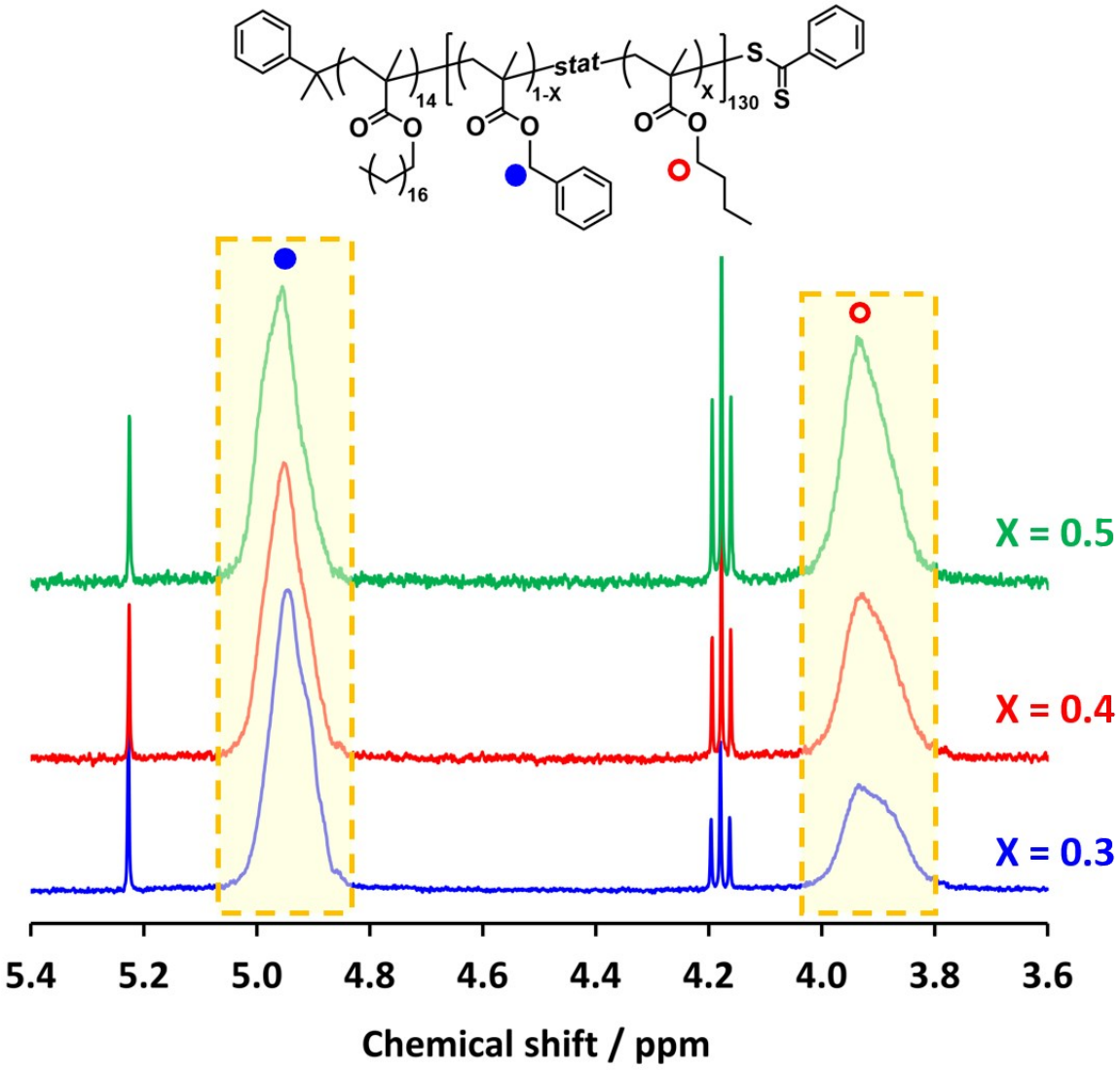

Fig. S4 ^{1}H NMR spectra showing the relative proportions of BuMA and BzMA repeat units within the structure-directing insoluble block for PSMA$_{14}$-P[(1-X)BzMA-*stat*-XBuMA]$_{130}$ nanoparticles for a target mole fraction, X, of 0.30 (blue trace), 0.40 (red trace) and 0.50 (green trace). The broad integral at 3.8 – 4.0 ppm corresponds to the two oxymethylene protons assigned to the BuMA repeat units and the integral at 4.8 – 5.1 ppm corresponds to the two oxymethylene protons of the BzMA repeat units (see **Fig. S3** for the fully assigned ^{1}H NMR spectrum).

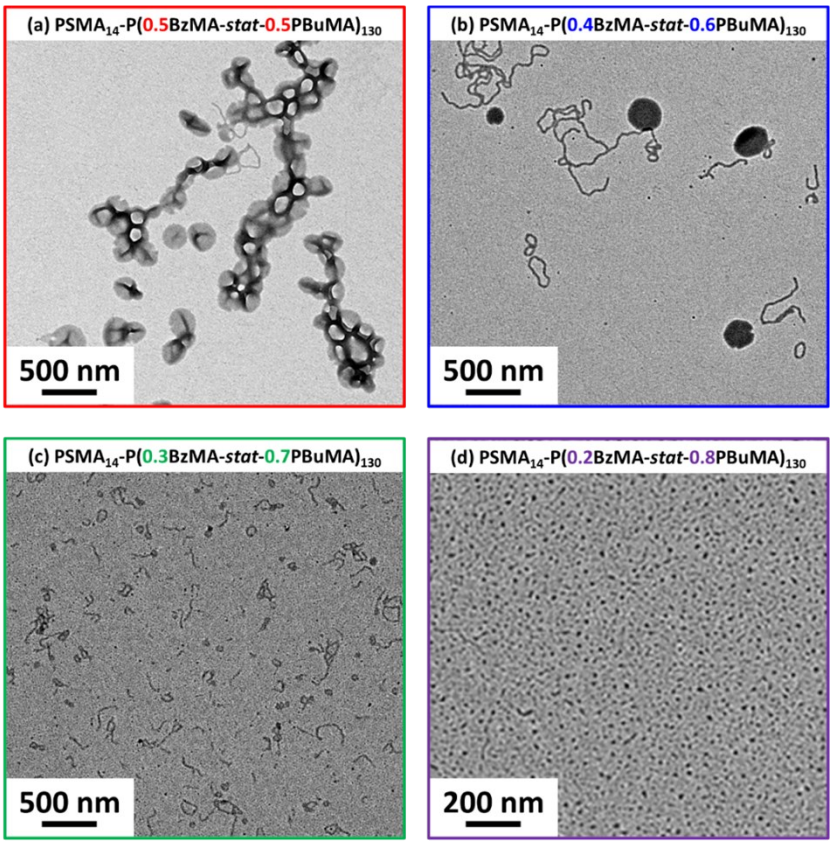

Fig. S5 Representative TEM images recorded at 20 °C for (a) $PSMA_{14}$-P(0.5BzMA-*stat*-0.5BuMA)$_{130}$ vesicles (plus a minor worm population), (b) a mixed phase comprising $PSMA_{14}$-P(0.4BzMA-*stat*-0.6BuMA)$_{130}$ vesicles and worms, (c) $PSMA_{14}$-P(0.3BzMA-*stat*-0.7BuMA)$_{130}$ worms and (d) $PSMA_{14}$-P(0.8BzMA-*stat*-0.2BuMA)$_{130}$ spheres.

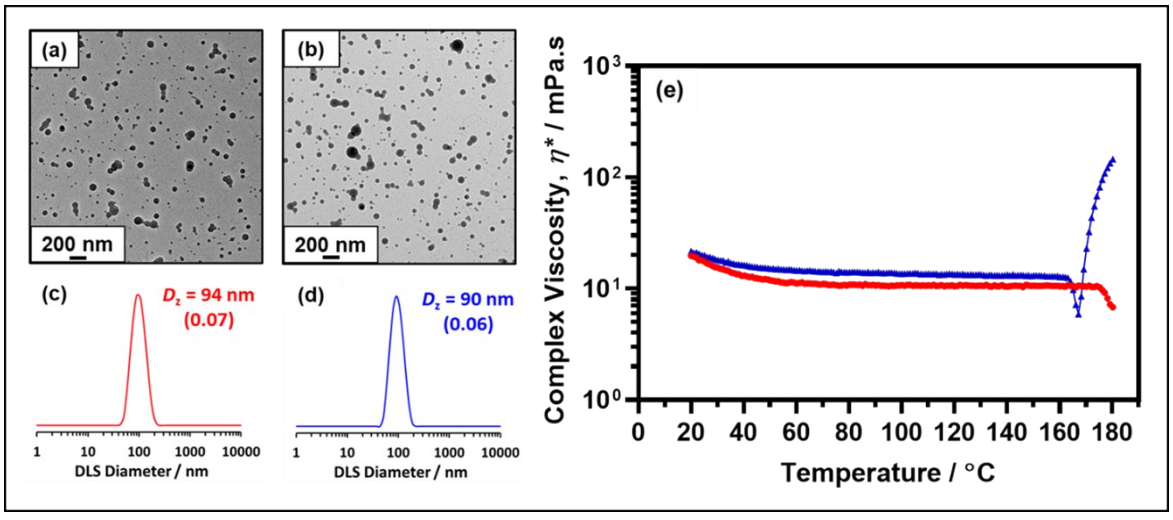

Fig. S6 Representative TEM images recorded at 20 °C for (a) $PSMA_{14}$-$PBzMA_{130}$ vesicles and (b) $PSMA_{14}$-$PBzMA_{125}$ vesicles. Particle size distributions and z-average diameters obtained by DLS for a 0.10% w/w dispersion of (c) $PSMA_{14}$-$PBzMA_{130}$ vesicles and (d) $PSMA_{14}$-$PBzMA_{125}$ vesicles. (e) Temperature dependence of the complex viscosity (η^*) observed for $PSMA_{14}$-$PBzMA_{130}$ nano-objects (red circles) and $PSMA_{14}$-$PBzMA_{130}$ nano-objects (blue triangles) on heating from 20 °C to 180 °C at 2°C min^{-1}. Data were obtained at 1.0 % strain using an angular frequency of 10 rad s^{-1}.

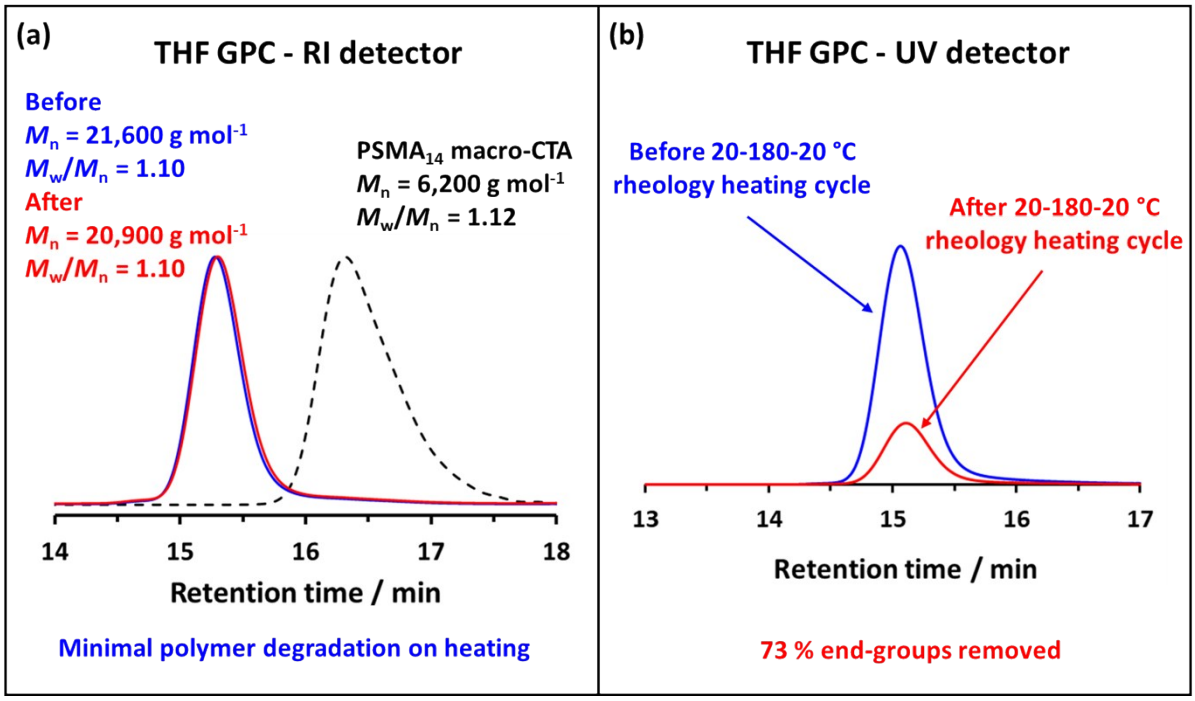

Fig. S7 THF GPC analysis of PSMA$_{14}$-P(0.5BzMA-*stat*-0.5BuMA)$_{130}$ chains before (blue traces) and after (red traces) subjecting a 10% w/w dispersion of such diblock copolymer nano-objects in mineral oil to a 20-180-20 °C thermal cycle in a rheology experiment. (a) Refractive index (RI) detector data with the PSMA$_{14}$ precursor included as a reference. (b) UV detector data at a fixed wavelength λ of 302 nm.

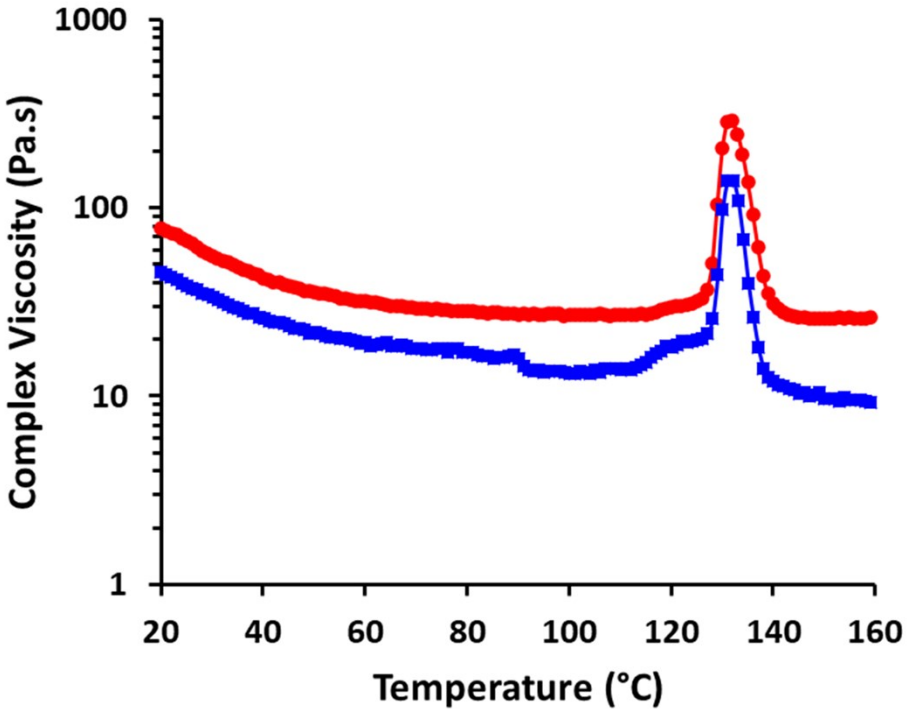

Fig. S8 Temperature dependence of the complex viscosity (η^*) observed for $PSMA_{14}$-P(0.5BzMA-*stat*-0.5BuMA)$_{130}$ nano-objects on heating from 20 °C to 160 °C. Red circles indicate data obtained for an 'as-synthesized' 10% w/w dispersion of $PSMA_{14}$-P(0.5BzMA-*stat*-0.5BuMA)$_{130}$ nano-objects prepared in mineral oil, (92% BuMA conversion, as determined by ^{1}H NMR spectroscopy). Blue squares indicate data obtained for an equivalent 10% w/w dispersion of $PSMA_{14}$-P(0.5BzMA-*stat*-0.5BuMA)$_{130}$ with post-polymerization addition of the equivalent of 8% residual BuMA (thus doubling the mass of residual BuMA comonomer that is present). Clearly, addition of further BuMA comonomer has minimal effect on the observed behavior.

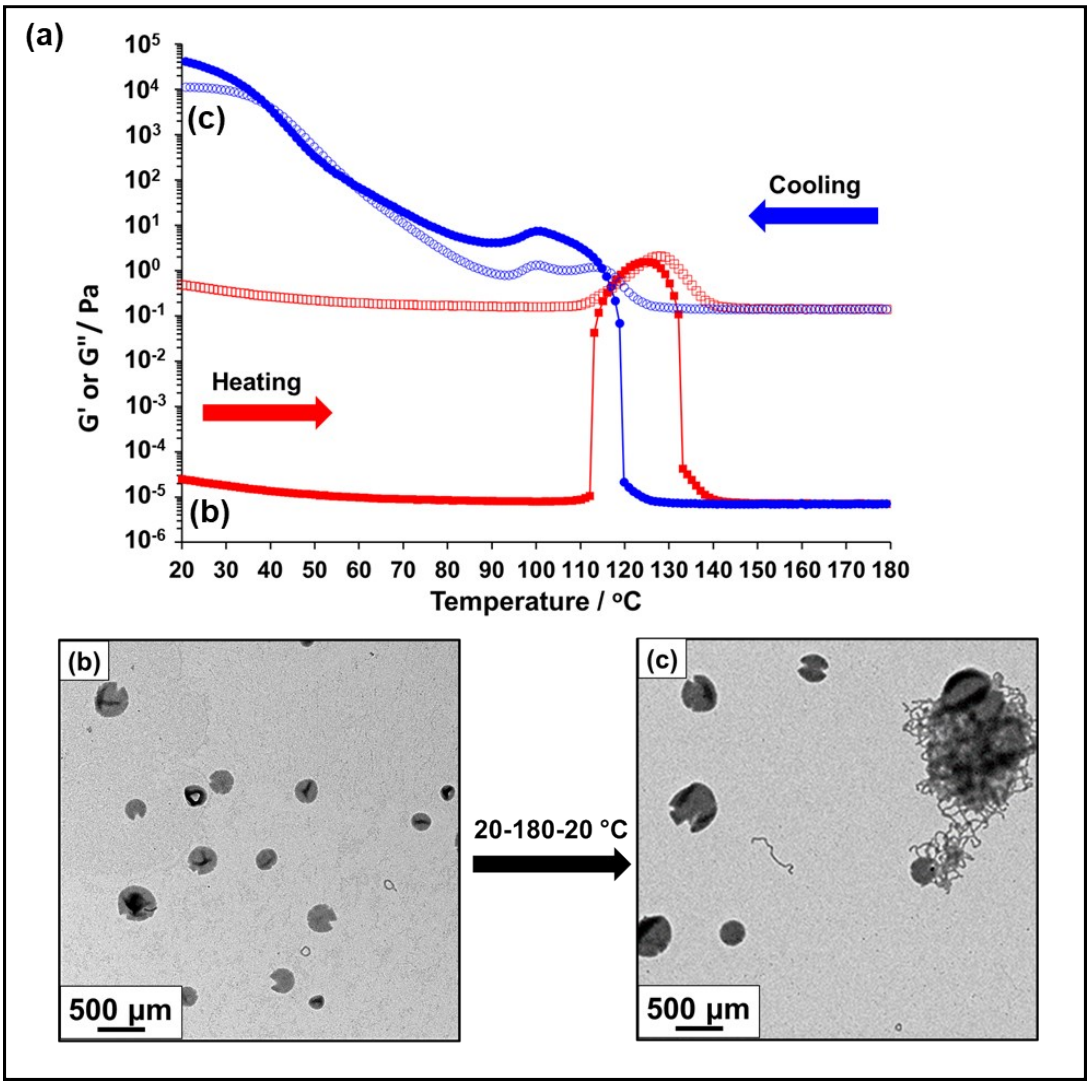

Fig. S9 (a) Temperature dependence of the storage modulus (*G'*, red filled squares) and loss modulus (*G''*, red empty squares) observed for a 10% w/w dispersion of $PSMA_{14}$-P(0.5BzMA-*stat*-0.5BuMA)$_{130}$ nano-objects in mineral oil when heating from 20 to 180 °C at 2 °C min^{-1}. The storage and loss moduli were also recorded on cooling the this dispersion from 180 °C to 20 °C at 2 °C min^{-1} (*G'* = blue filled circles and *G''* = blue empty circles). This experiment was conducted at 1.0% strain and a constant angular frequency of 10 rad s^{-1}. Representative TEM images recorded after drying 0.10% w/w dispersions of $PSMA_{14}$-P(0.5BzMA-*stat*-0.5BuMA)$_{130}$ nano-objects at 20 °C (b) before and (c) after this 20-180-20 °C thermal cycle.

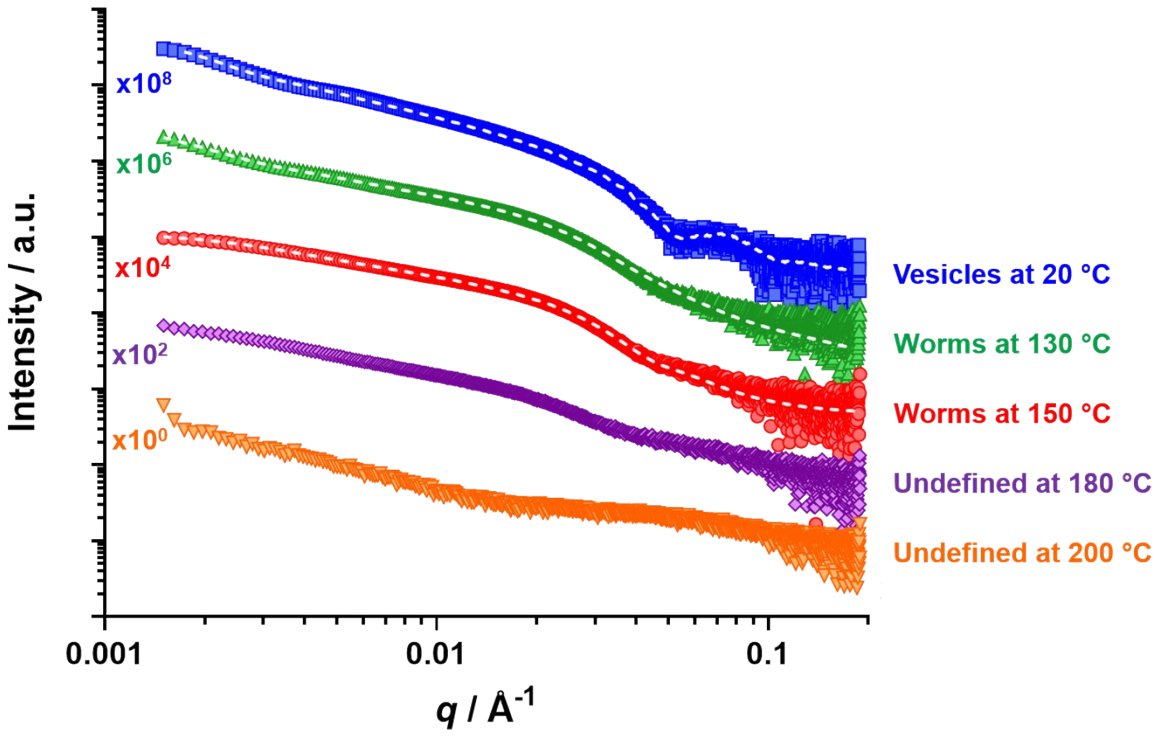

Fig. S10 Representative SAXS patterns recorded for $PSMA_{14}$-P(0.5BzMA-*stat*-0.5BuMA)$_{130}$ nano-objects at 20 °C, 130 °C and 150 °C, with dashed lines indicating the data fits obtained using the relevant scattering model (as shown in Fig. 9). The patterns recorded at 180 °C and 200 °C could not be satisfactorily fitted using any of the scattering models presented herein.